



## Journal of Coordination Chemistry

Publication details, including instructions for authors and subscription information:

<http://www.tandfonline.com/loi/gcoo20>

### Mn(III) complex supported on Fe<sub>3</sub>O<sub>4</sub> nanoparticles: magnetically separable nanocatalyst for selective oxidation of thiols to disulfides

Mojtaba Bagherzadeh<sup>a</sup>, Mohammad Mehdi Haghdoost<sup>a</sup>, Firouz Matloubi Moghaddam<sup>a</sup>, Behzad Koushki Foroushani<sup>a</sup>, Setareh Saryazdi<sup>a</sup> & Ebrahim Payab<sup>a</sup>

<sup>a</sup> Chemistry Department, Sharif University of Technology, Tehran, Iran.

Accepted author version posted online: 04 Jul 2013.

To cite this article: Mojtaba Bagherzadeh, Mohammad Mehdi Haghdoost, Firouz Matloubi Moghaddam, Behzad Koushki Foroushani, Setareh Saryazdi & Ebrahim Payab (2013) Mn(III) complex supported on Fe<sub>3</sub>O<sub>4</sub> nanoparticles: magnetically separable nanocatalyst for selective oxidation of thiols to disulfides, Journal of Coordination Chemistry, 66:17, 3025-3036, DOI: [10.1080/00958972.2013.821699](http://dx.doi.org/10.1080/00958972.2013.821699)

To link to this article: <http://dx.doi.org/10.1080/00958972.2013.821699>

PLEASE SCROLL DOWN FOR ARTICLE

Taylor & Francis makes every effort to ensure the accuracy of all the information (the "Content") contained in the publications on our platform. However, Taylor & Francis, our agents, and our licensors make no representations or warranties whatsoever as to the accuracy, completeness, or suitability for any purpose of the Content. Any opinions and views expressed in this publication are the opinions and views of the authors, and are not the views of or endorsed by Taylor & Francis. The accuracy of the Content should not be relied upon and should be independently verified with primary sources of information. Taylor and Francis shall not be liable for any losses, actions, claims, proceedings, demands, costs, expenses, damages, and other liabilities whatsoever or howsoever caused arising directly or indirectly in connection with, in relation to or arising out of the use of the Content.

This article may be used for research, teaching, and private study purposes. Any substantial or systematic reproduction, redistribution, reselling, loan, sub-licensing, systematic supply, or distribution in any form to anyone is expressly forbidden. Terms &



## Mn(III) complex supported on Fe<sub>3</sub>O<sub>4</sub> nanoparticles: magnetically separable nanocatalyst for selective oxidation of thiols to disulfides

MOJTABA BAGHERZADEH\*, MOHAMMAD MEHDI HAGHDOOST,  
FIROUZ MATLOUBI MOGHADDAM, BEHZAD KOUSHKI FOROUSHANI,  
SETAREH SARYAZDI and EBRAHIM PAYAB

Chemistry Department, Sharif University of Technology, Tehran, Iran

(Received 3 March 2013; in final form 21 June 2013)

A manganese(III) complex, [Mn(phox)<sub>2</sub>(CH<sub>3</sub>OH)<sub>2</sub>]ClO<sub>4</sub> (phox = 2-(2'-hydroxyphenyl)oxazoline), was immobilized on silica-coated magnetic Fe<sub>3</sub>O<sub>4</sub> nanoparticles through the amino propyl linkage using a grafting process in dichloromethane. The resulting Fe<sub>3</sub>O<sub>4</sub>@SiO<sub>2</sub>-NH<sub>2</sub>@Mn(III) nanoparticles are used as efficient and recyclable catalysts for selective oxidation of thiols to disulfides using urea-hydrogen peroxide as the oxidant. The nanocatalyst was recycled several times. Leaching and recycling experiments revealed that the nanocatalyst can be recovered, recycled, and reused more than five times, without the loss of catalytic activity and magnetic properties. The recycling of the nanocatalyst in six consecutive runs afforded a total turnover number of more than 10,000. The heterogeneous Fe<sub>3</sub>O<sub>4</sub>@SiO<sub>2</sub>-NH<sub>2</sub>@Mn(III) nanoparticle shows more selectivity for the formation of disulfides in comparison with the homogeneous manganese complex.

**Keywords:** Mn(III) complex; Fe<sub>3</sub>O<sub>4</sub> nanoparticle; Magnetically separable nanocatalyst; Thiol oxidation; Disulfides

### 1. Introduction

Synthesizing catalysts with the desired properties is a highly sought-after and challenging goal. A number of catalysts with various characteristics have been developed [1]. Homogeneous catalysts typically operate at relatively mild conditions and exhibit high activities and selectivities, but it is difficult to separate and regenerate the catalyst from the reaction mixture. Covalent grafting of a homogeneous catalyst on solid supports [2] results in relatively good outcomes, but decreases the active surface area and the reactivity of immobilized catalysts.

Immobilized homogeneous catalysis has gained a new impulse with the advent of nanotechnology [3]. Because of the large surface area of nanoparticles, high loadings of catalytically active sites are guaranteed and, therefore, nanoparticle-supported homogeneous catalysts exhibit high catalytic activity and selectivity [4]. However, nanometer-sized particles are difficult to separate by traditional filtration techniques and expensive

\*Corresponding author. Email: [bagherzadeh@sharif.edu](mailto:bagherzadeh@sharif.edu)

ultracentrifugation is often needed to have good separation of the catalyst from the reaction mixture. This shortcoming could be obviated using magnetic nanoparticle (MNP) supports. An external magnet could easily separate the immobilized catalysts from the reaction mixture, which results in more effective separation than conventional methods [4–10].

We have focused on using magnetically separable transition metal complexes as catalysts for the synthesis of organic compounds [11]. In this paper, we synthesized the first magnetically recyclable manganese complex through covalent anchoring of  $[\text{Mn}(\text{phox})_2(\text{CH}_3\text{OH})_2]\text{ClO}_4$  ( $\text{phox} = 2\text{-(2'-hydroxyphenyl)oxazoline}$ ) on silica-coated  $\text{Fe}_3\text{O}_4$  nanoparticles. This catalyst (hereafter called  $\text{Fe}_3\text{O}_4@\text{SiO}_2\text{-NH}_2@\text{Mn(III)}$ ) efficiently catalyzes the selective oxidation of thiols to disulfides using urea-hydrogen peroxide (UHP) as the environmental-friendly oxidant. In addition, the present  $\text{Fe}_3\text{O}_4@\text{SiO}_2\text{-NH}_2@\text{Mn(III)}$  catalyst was easily recovered and reused without the loss of activity or selectivity.

## 2. Experimental

### 2.1. Methods

The  $^1\text{H}$  NMR spectra were recorded at room temperature with a Bruker FT NMR 500 (500 MHz) spectrophotometer using  $\text{CDCl}_3$  as solvent and chemical shifts were reported in ppm with tetramethylsilane as an internal standard. Scanning electron microscopy (SEM) was carried out on Philips XL30. IR spectra were recorded as KBr pellets using a ABB FT-IR spectrophotometer. Measures of pH were carried out by a Mettler Toledo S40 SevenMulti<sup>TM</sup> pH-meter. A Varian (AA220) flame atomic absorption spectrometer (air/acetylene flame) was used for the determination of manganese ion. A Hewlett-Packard (HP, Palo Alta, USA) HP 6890 plus series GC equipped with a split/splitless injector and a HP 5973 mass-selective detector system were used for GC-MS analysis. The MS was operated in the EI mode (70 eV) and separations were performed on a  $30\text{ m} \times 0.25\text{ mm}$  HP-5 MS column (0.25  $\mu\text{m}$  film thickness). The UV-Vis DRS spectra of the samples were recorded with a PE Lambda 20 spectrometer.

### 2.2. Synthesis of $[\text{Mn}(\text{phox})_2(\text{CH}_3\text{OH})_2]\text{ClO}_4$ complex

Hphox (2-(2'-hydroxyphenyl)oxazoline) was prepared in a similar manner according to the reported procedure [12]. Manganese complexes, bis[2-(2'-hydroxyphenyl)-oxazolinato] dimethanol manganese(III) perchlorate,  $[\text{Mn}(\text{phox})_2(\text{CH}_3\text{OH})_2]\text{ClO}_4$  were synthesized according to previously reported work [13].

### 2.3. Synthesis of $\text{Fe}_3\text{O}_4$ nanoparticles

Under  $\text{N}_2$ , 2 g (10.0 mM) of  $\text{FeCl}_2 \cdot 4\text{H}_2\text{O}$ , 5.2 g (19.3 mM) of  $\text{FeCl}_3 \cdot 6\text{H}_2\text{O}$ , and 0.85 mL of concentrated HCl were dissolved in 25 mL of degassed water. This solution was added dropwise at room temperature to 250 mL of sodium hydroxide solution (1.5 M) under  $\text{N}_2$ . After the mixture was stirred for 30 min (1300 rpm), the formed black precipitates were separated using a 0.5 T magnet and washed several times with degassed water. Finally, for storage of MNPs,  $\text{Fe}_3\text{O}_4$  nanoparticles were dispersed in 100 mL degassed water under  $\text{N}_2$  [14].

#### 2.4. Synthesis of Fe<sub>3</sub>O<sub>4</sub>@SiO<sub>2</sub> nanoparticles

One gram of freshly prepared Fe<sub>3</sub>O<sub>4</sub> nanoparticles was added to 30 mL of an aqueous solution of citric acid (0.02 g/mL), then the pH was adjusted to 5.2 using ammonia and the mixture was heated to 80–90 °C for 1.5 h. After heating, the pH of the reaction mixture was increased with ammonia to pH=11, and 1.25 mL of tetraethylorthosilicate (TEOS) dissolved in ethanol (12.5 mL) was added dropwise into the suspension of particles. The mixture was stirred at room temperature for 24 h to let the base-catalyzed hydrolysis and the condensation of TEOS monomers on the nanoparticles surface go to completion. Finally, the dark brown Fe<sub>3</sub>O<sub>4</sub>@SiO<sub>2</sub> nanoparticles were separated using a magnet and were washed with distilled water and ethanol.

#### 2.5. Synthesis of Fe<sub>3</sub>O<sub>4</sub>@SiO<sub>2</sub>-NH<sub>2</sub>

Five milliliter of 3-aminopropyltriethoxysilane (APS) dissolved in 100 mL ethanol was added dropwise to the suspension of one gram of silica-coated Fe<sub>3</sub>O<sub>4</sub> nanoparticles in 100 mL of distilled water. The pH of the reaction mixture was increased with KOH to pH=11 and the reaction mixture was stirred at 70 °C for 5 h. Finally, the brown precipitates were separated using a 0.5 T magnet and were thoroughly washed with distilled water (five times, 150 mL) to remove any unbound APS.

#### 2.6. Synthesis of Fe<sub>3</sub>O<sub>4</sub>@SiO<sub>2</sub>-NH<sub>2</sub>@Mn(III) nanoparticles

Under N<sub>2</sub>, one gram of Fe<sub>3</sub>O<sub>4</sub>@SiO<sub>2</sub>-NH<sub>2</sub> nanoparticles was added to a solution of [Mn(phox)<sub>2</sub>(CH<sub>3</sub>OH)<sub>2</sub>]ClO<sub>4</sub> complex (100 mg) in 100 mL of dry dichloromethane and the suspension was refluxed for 24 h. After cooling, the brown Fe<sub>3</sub>O<sub>4</sub>@SiO<sub>2</sub>-NH<sub>2</sub>@Mn(III) nanoparticles were separated using a magnet and were washed several times with dichloromethane and toluene.

#### 2.7. General conditions for catalytic oxidation of thiols

A typical reaction using the Fe<sub>3</sub>O<sub>4</sub>@SiO<sub>2</sub>-NH<sub>2</sub>@Mn(III) nanoparticles as catalyst and thiols as substrate is described as follows. To a solution of thiol (1 mM) and catalyst (0.01 g, containing 0.0002 mM of manganese complex) in a (1:1) mixture of CH<sub>3</sub>OH-CH<sub>2</sub>Cl<sub>2</sub> (2 mL) was added UHP (0.093 g, 1 mM) as the oxidant. The mixture was stirred at room temperature for 2 h. The catalyst particles were then collected at the bottom of the test tube using a magnet, the supernatant was carefully decanted, and the completion of oxidation reaction was followed by TLC (petroleum ether/ethyl acetate, 4:1). After the separation of catalyst nanoparticles, the solvent supernatant was removed under vacuum and the remaining was purified by column chromatography using petroleum ether/ethylacetate, 4:1. Isolated products were weighted and also analyzed by <sup>1</sup>H NMR. Washing several times with methanol and dichloromethane, the catalyst particles were dried in vacuum and could be reused.

### 3. Results and discussion

The methodologies used in functionalization of Fe<sub>3</sub>O<sub>4</sub> nanoparticle surfaces and subsequent Mn(III) complex anchoring are presented in scheme 1. We started with Fe<sub>3</sub>O<sub>4</sub>



Scheme 1. Step-by-step synthesis of  $\text{Fe}_3\text{O}_4@\text{SiO}_2\text{-NH}_2@\text{Mn(III)}$ .

nanoparticles of 10–50 nm average diameters which were prepared by facile and convenient co-precipitation method [14]. The SEM image of the dispersed MNPs in water depicts relatively uniform  $\text{Fe}_3\text{O}_4$  nanoparticles with dimensions less than 50 nm and rather high surface area (Supplementary material). The high surface area of nanoparticles is beneficial for the high loading of catalyst during the complex anchoring step.

In the XRD pattern of the prepared  $\text{Fe}_3\text{O}_4$  (figure 1), six characteristic peaks ( $2\theta = 30.1$ ,  $35.7$ ,  $43.1$ ,  $54.0$ ,  $57.1$ , and  $63.6$ ), corresponding to (220), (311), (400), (422), (511), and (440) Bragg reflections, respectively, were observed. These peaks are consistent with the database in JCPDS file (PCPDFWIN v.2.02, PDF No. 85-1436) and reveal that the resultant nanoparticles were pure  $\text{Fe}_3\text{O}_4$  without impurity phases. The average particle size of the sample was estimated by Scherrer's equation to be 15.9, which is in good agreement with that observed in the SEM image (Supplementary material).

Although  $\text{Fe}_3\text{O}_4$  nanoparticles can be easily prepared, they have the following disadvantage of being fairly reactive to acidic and oxidative environments [15]. In the presence of oxygen, the  $\text{Fe}_3\text{O}_4$  nanoparticles rapidly oxidize to  $\text{Fe}_2\text{O}_3$  which shows low magnetic properties [16]. Also, direct grafting of metal complex on the surface of  $\text{Fe}_3\text{O}_4$  nanoparticles is almost impossible due to relative inertness of the surface. There are only a limited number of molecules that can be bonded to MNP surfaces [17]. Freshly prepared  $\text{Fe}_3\text{O}_4$  nanoparticles will aggregate rapidly into large clusters and thus will lose their nano properties [4]. In order to prevent these problems, the nanoparticles have to be coated. Among various coating agents, silica offers unique advantages for applications, particularly, in catalysis. For doing so, the silica-coated MNPs ( $\text{Fe}_3\text{O}_4@\text{SiO}_2$ ) were

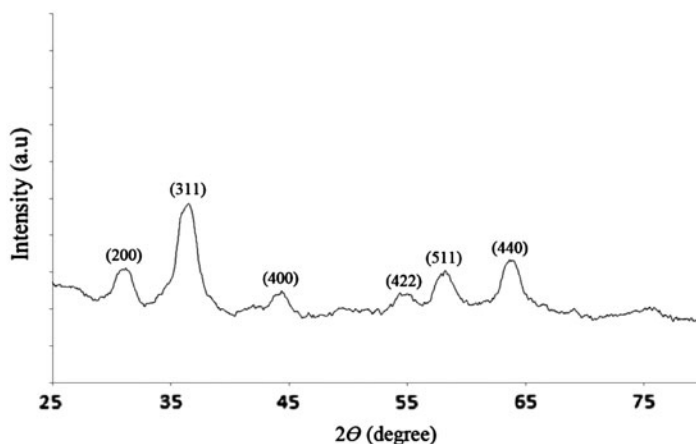


Figure 1. XRD patterns of the as-synthesized  $\text{Fe}_3\text{O}_4$  nanoparticles.

synthesized by basic hydrolysis and condensation of TEOS on the surface of the Fe<sub>3</sub>O<sub>4</sub> nanoparticles [17]. The obtained Fe<sub>3</sub>O<sub>4</sub> and Fe<sub>3</sub>O<sub>4</sub>@SiO<sub>2</sub> nanoparticles were characterized in our previous work [11].

In previous work, a vanadium complex was covalently grafted via the reaction of chloro complex and silanol groups of surface with concomitant release of HCl [11]. Presence of a halide on metal center, which is a necessity in this process, is limited to a few complexes. A possible way to overcome this drawback is the surface derivatization with a variety of functional groups. One of the preferred functional groups for bonding different metal centers to nanoparticles is NH<sub>2</sub>. In this work, Fe<sub>3</sub>O<sub>4</sub>@SiO<sub>2</sub> nanoparticles were functionalized by bonding 3-aminopropylsilane (APS) to their surfaces as described elsewhere [17]. Because of the presence of the magnetic core inside, MNPs cannot be analyzed by solid-state NMR spectroscopy. Therefore, amino-functionalized nanoparticles (Fe<sub>3</sub>O<sub>4</sub>@SiO<sub>2</sub>-NH<sub>2</sub>) were characterized by FT-IR and elemental analysis. Figure 2 shows the FT-IR spectra of the core-shell MNPs before and after being functionalized with APS. Compared with the FT-IR spectrum of Fe<sub>3</sub>O<sub>4</sub>@SiO<sub>2</sub>, the characteristic peaks at 2861 and 2926 cm<sup>-1</sup> ascribed to C-H stretch of the propyl in the pendant APS can be clearly observed in the FT-IR spectrum of Fe<sub>3</sub>O<sub>4</sub>@SiO<sub>2</sub>-NH<sub>2</sub>, which confirms that APS molecules have bonded to the surface of the silica-coated MNPs [18]. This conclusion is further supported by elemental analysis which gave the percentages of C, H, and N to be 5.10, 1.54, and 1.53%, respectively. The wave numbers of N-H asymmetric and symmetric stretching vibrations of the amine group are at 3300–3400 cm<sup>-1</sup> and are obscured by water bands [19].

The SEM image of Fe<sub>3</sub>O<sub>4</sub>@SiO<sub>2</sub>-NH<sub>2</sub> nanoparticles, as shown in figure 3, clearly suggests a smooth morphology and confirms that the particles fall in the nano size range after silica coating and amine functionalization. Comparison of the SEM image of these nanoparticles with those of bare Fe<sub>3</sub>O<sub>4</sub> (Supplementary material) reveals that Fe<sub>3</sub>O<sub>4</sub>@SiO<sub>2</sub>-NH<sub>2</sub> exhibits particles having smooth surfaces, while the Fe<sub>3</sub>O<sub>4</sub> particles exhibit rough surfaces. It must be emphasized that the smoothness of the surface is due to the presence of silica shell on the particles. This comparison also shows that the final Fe<sub>3</sub>O<sub>4</sub>@SiO<sub>2</sub>-NH<sub>2</sub> nanoparticle size is very close to the size of the initial Fe<sub>3</sub>O<sub>4</sub> particles, indicating that the silica layer is very thin.

After functionalization by APS, Fe<sub>3</sub>O<sub>4</sub>@SiO<sub>2</sub>-NH<sub>2</sub> nanoparticles offer NH<sub>2</sub> binding sites for immobilization of many metal complexes. We treated Fe<sub>3</sub>O<sub>4</sub>@SiO<sub>2</sub>-NH<sub>2</sub> nanoparticles with the [Mn(phox)<sub>2</sub>(CH<sub>3</sub>OH)<sub>2</sub>]ClO<sub>4</sub> complex in dry CH<sub>2</sub>Cl<sub>2</sub> to synthesize Fe<sub>3</sub>O<sub>4</sub>@SiO<sub>2</sub>-NH<sub>2</sub>@Mn(III) nanoparticles. Methanols in the axial positions are highly labile toward

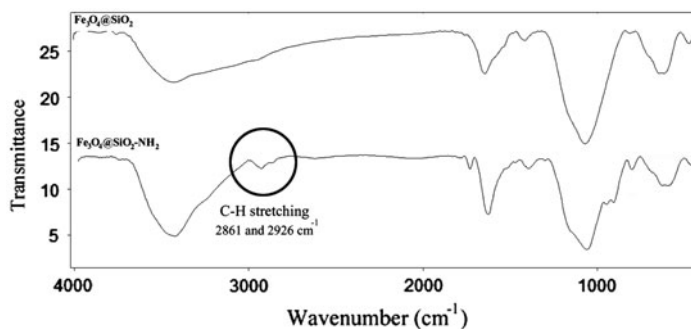


Figure 2. FT-IR spectra of Fe<sub>3</sub>O<sub>4</sub>@SiO<sub>2</sub> (up) and Fe<sub>3</sub>O<sub>4</sub>@SiO<sub>2</sub>-NH<sub>2</sub> (down) nanoparticles.



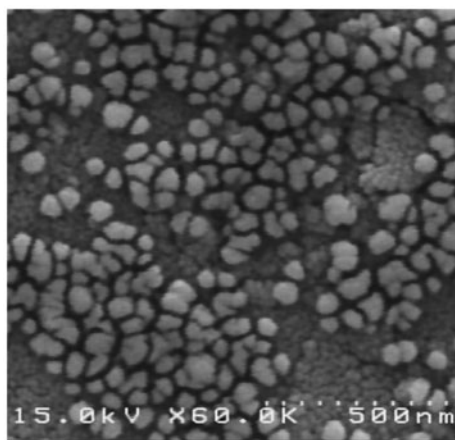


Figure 3. SEM image of the  $\text{Fe}_3\text{O}_4@\text{SiO}_2\text{-NH}_2$  nanoparticles.

substitution. Therefore, we proposed that methanol axial ligands of the complex could be replaced by the amine group of the surface, which is a stronger nucleophile than methanol. Comparison of the FT-IR spectra of  $[\text{Mn}(\text{phox})_2(\text{CH}_3\text{OH})_2]\text{ClO}_4$  complex [figure 4(a)] with those of the  $\text{Fe}_3\text{O}_4@\text{SiO}_2\text{-NH}_2@\text{Mn}(\text{III})$  nanoparticles [figure 4(b)] revealed that signals at 758, 868, 932, 1332, 1399, 1477, and  $1541\text{ cm}^{-1}$  corresponding to the vibration modes of manganese complex are present in the FT-IR spectra of  $\text{Fe}_3\text{O}_4@\text{SiO}_2\text{-NH}_2@\text{Mn}(\text{III})$  nanoparticles.

Figure 5 shows the diffuse reflectance UV-Vis (DRS) spectrum of freshly prepared  $\text{Fe}_3\text{O}_4@\text{SiO}_2\text{-NH}_2@\text{Mn}(\text{III})$  nanoparticles (curve c). The UV-Vis spectra of the  $[\text{Mn}(\text{phox})_2(\text{CH}_3\text{OH})_2]\text{ClO}_4$  complex in methanol solution are given for comparison (curve a). The curve of manganese complex in methanol solution exhibits ligand-to-metal charge transfer and  $\pi \rightarrow \pi^*$  transition with absorption maxima around 289 and 237 nm, respectively [13]. The DRS spectrum of the  $\text{Fe}_3\text{O}_4@\text{SiO}_2\text{-NH}_2@\text{Mn}(\text{III})$  nanoparticles shows comparable absorption behavior, but exhibits a slight red shift due to the interaction of the metal complex with the surface.

The thermal behavior of the  $\text{Fe}_3\text{O}_4@\text{SiO}_2\text{-NH}_2@\text{Mn}(\text{III})$  nanoparticles was evaluated by TG-DTA. The TGA and DTA curves shown in Supplementary material indicate the weight loss of  $\text{Fe}_3\text{O}_4@\text{SiO}_2\text{-NH}_2@\text{Mn}(\text{III})$  nanoparticles is a multistage process that

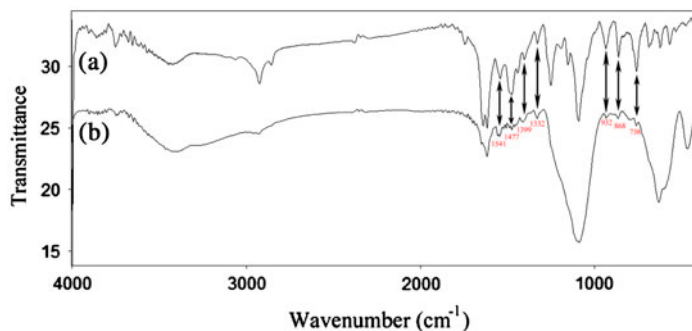


Figure 4. FT-IR spectra of (a)  $[\text{Mn}(\text{phox})_2(\text{CH}_3\text{OH})_2]\text{ClO}_4$  and (b)  $\text{Fe}_3\text{O}_4@\text{SiO}_2\text{-NH}_2@\text{Mn}(\text{III})$  nanoparticles.



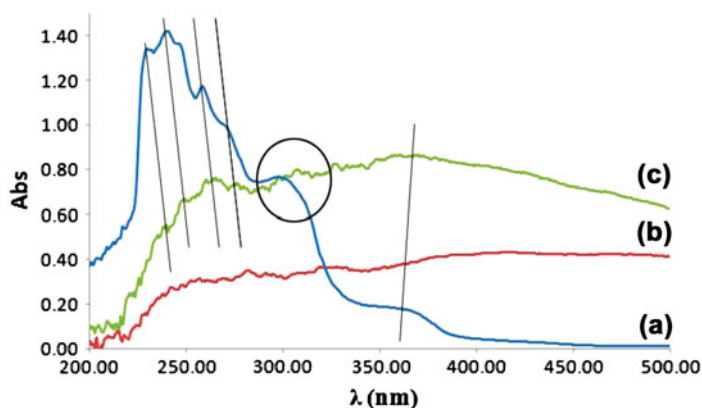


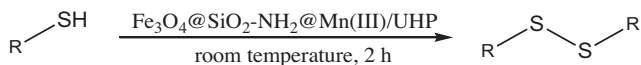
Figure 5. (a) The UV-Vis spectrum of  $[\text{Mn}(\text{phox})_2(\text{CH}_3\text{OH})_2]\text{ClO}_4$ , (b) diffuse reflectance UV-Vis spectrum of  $\text{Fe}_3\text{O}_4@\text{SiO}_2\text{-NH}_2$ , and (c) diffuse reflectance UV-Vis spectrum of  $\text{Fe}_3\text{O}_4@\text{SiO}_2\text{-NH}_2@\text{Mn(III)}$  nanoparticles.

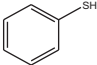
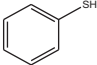
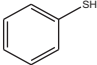
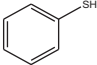
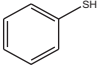
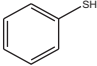
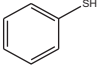
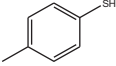
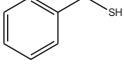
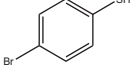
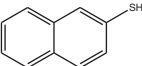
corresponds to three peaks in the DTA curves. In the first step, the nanoparticles show a small weight loss of 3.38% from 50 to 150 °C, mainly due to the loss of physically adsorbed water. The second and third weight loss peaks at 300–600 °C are due to the loss of organic groups (phox and amino propyl linkage).

The FT-IR, UV-Vis, and TGA studies provide evidence for anchoring of the manganese(III) complex. Elemental analysis of  $\text{Fe}_3\text{O}_4@\text{SiO}_2\text{-NH}_2@\text{Mn(III)}$  nanoparticles gave the percentages of carbon and nitrogen to be 6.01 and 1.59%, respectively. The significant increase in C/N ratio from 3.3 in  $\text{Fe}_3\text{O}_4@\text{SiO}_2\text{-NH}_2$  to 3.7 in  $\text{Fe}_3\text{O}_4@\text{SiO}_2\text{-NH}_2@\text{Mn(III)}$  strongly justifies this conclusion that complex immobilization has been successful. The loading of manganese(III) complex was  $0.0208 \text{ mM g}^{-1}$ , determined by AAS test of manganese after acid digestion.

Selective oxidation of sulfur-containing organic molecules, such as thiols and sulfides, without the formation of over-oxidized products is one of the most important transformations in total synthesis, biological chemistry, and petroleum industries, and it has recently received attention from several research groups [20–30]. These considerations led us to test the  $\text{Fe}_3\text{O}_4@\text{SiO}_2\text{-NH}_2@\text{Mn(III)}$  nanocatalyst as a magnetically recyclable catalyst for selective oxidation of thiols to disulfides (table 1). As proof of principle, 0.01 g of  $\text{Fe}_3\text{O}_4@\text{SiO}_2\text{-NH}_2@\text{Mn(III)}$  nanocatalyst (0.0002 mM of manganese loading) was tested. Catalysis in  $\text{CH}_2\text{Cl}_2/\text{MeOH}$  using 1 mM of both thiophenol and UHP was run to selectively oxidize thiophenol to diphenyldisulfide in 90% yield (table 1, entry 5). Several thiols, such as 4-methylthiophenol (table 1, entry 8), benzylthiol (table 1, entry 9), 4-bromothiophenol (table 1, entry 10), and naphthalenethiol (table 1, entry 11), underwent oxidation and produced the corresponding symmetric disulfides. In all cases, only selective formation of disulfides was observed and no thiolsulfonate, an over-oxidized side product, was detected.

The heterogeneous  $\text{Fe}_3\text{O}_4@\text{SiO}_2\text{-NH}_2@\text{Mn(III)}$  nanoparticle is a more selective catalyst than the homogeneous  $[\text{Mn}(\text{phox})_2(\text{CH}_3\text{OH})_2]\text{ClO}_4$  complex (table 1, entry 5 *versus* 6). Oxidation with  $[\text{Mn}(\text{phox})_2(\text{CH}_3\text{OH})_2]\text{ClO}_4$  proceeded with a 55% yield of disulfides accompanied by a significant amount of a side product (table 1, entries 6 and 7). The structure of the side product was established as  $\alpha$ -diphenyldisulfone on the basis of elemental analysis and GC-MS (Supplementary material). Diphen is one of the various possible oxidized forms of disulfides that still retain the S-S bond (scheme 2) [31]. It is

Table 1. Oxidation of thiols by  $\text{Fe}_3\text{O}_4@\text{SiO}_2\text{-NH}_2@\text{Mn(III)}$  nanocatalyst.<sup>a</sup>

Entry	Thiol	Catalyst	Yield (%) <sup>b</sup>	Selectivity to disulfide (%)	Melting point of product (°C) <sup>c</sup>
1		—	Trace	—	—
2		$\text{Fe}_3\text{O}_4$	Trace	—	—
3		$\text{Fe}_3\text{O}_4@\text{SiO}_2$	Trace	—	—
4		$\text{Fe}_3\text{O}_4@\text{SiO}_2\text{-NH}_2$	Trace	—	—
5		$\text{Fe}_3\text{O}_4@\text{SiO}_2\text{-NH}_2@\text{Mn(III)}$	90	100	59–61 (59–60)
6		$[\text{Mn}(\text{phox})_2(\text{CH}_3\text{OH})_2]\text{ClO}_4$	54 <sup>c</sup>	80	59–61 (59–60)
7		$[\text{Mn}(\text{phox})_2(\text{CH}_3\text{OH})_2]\text{ClO}_4$	55 <sup>d</sup>	82	59–61 (59–60)
8		$\text{Fe}_3\text{O}_4@\text{SiO}_2\text{-NH}_2@\text{Mn(III)}$	83	100	53–54 (52–56)
9		$\text{Fe}_3\text{O}_4@\text{SiO}_2\text{-NH}_2@\text{Mn(III)}$	81	100	67–69 (69–70)
10		$\text{Fe}_3\text{O}_4@\text{SiO}_2\text{-NH}_2@\text{Mn(III)}$	88	100	91–93 (91–93)
11		$\text{Fe}_3\text{O}_4@\text{SiO}_2\text{-NH}_2@\text{Mn(III)}$	87	100	141–143 (142–145)

<sup>a</sup>Reaction conditions: thiol (1 mM), UHP (1 mM), catalyst (0.01 g, 0.0002 mM of Mn(III) complex), 2 mL solvent ( $\text{CH}_2\text{Cl}_2\text{-CH}_3\text{OH}$  (1 : 1 v/v)), and room temperature, 2 h.

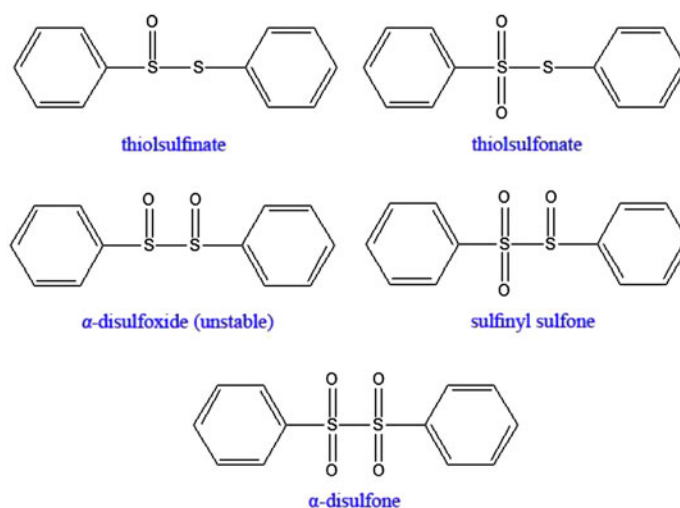
<sup>b</sup>All yields refer to isolated yields.

<sup>c</sup>0.025 mM of catalyst were employed.

<sup>d</sup>0.05 mM of catalyst were employed.

<sup>e</sup>Values in parentheses are the melting points reported [32, 33].

obvious that the formation of this over-oxidized product could be responsible for the low yield of disulfide in Mn(III) homogeneous catalytic system. Direct oxidation of disulfides to disulfones has not been reported until now.

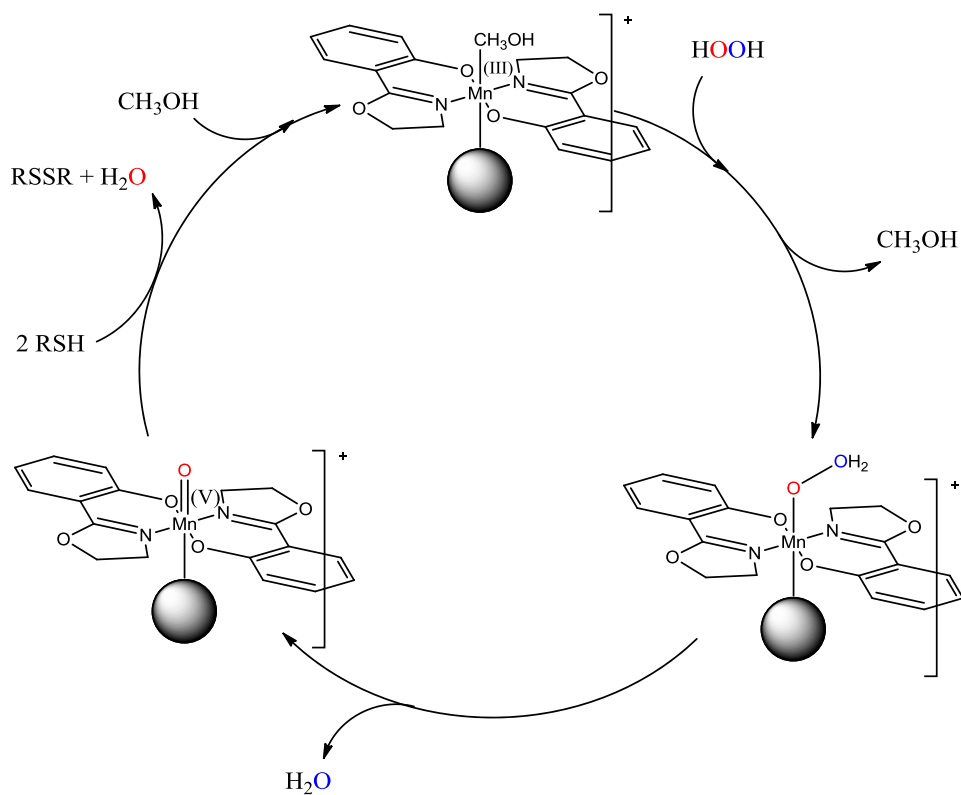


Scheme 2. Various oxidized forms of diphenyldisulfide.

Control experiments indicate that no oxidation occurred in the absence of catalyst (table 1, entry 1). The use of  $\text{Fe}_3\text{O}_4$ ,  $\text{Fe}_3\text{O}_4@\text{SiO}_2$ , and  $\text{Fe}_3\text{O}_4@\text{SiO}_2\text{-NH}_2$  nanoparticles in place of  $\text{Fe}_3\text{O}_4@\text{SiO}_2\text{-NH}_2@\text{Mn(III)}$  led to the formation of the disulfide in very poor yield and selectivity (table 1, entries 2–4).

Based on previously reported studies [25, 34], it is possible to postulate two mechanisms for the catalytic oxidation of thiols to disulfides. In the first mechanism, the catalytic reaction is mediated by one-electron reduction of the manganese complex, resulting in the formation of Mn(II) intermediate and thiol radical [25]. The formation of S–S bond is likely to take place via coupling of thiol radicals. The Mn(III) complex is then regenerated with the reaction of Mn(II) intermediate and UHP, which re-enters the cycle. To test the validity of this mechanism, a catalytic run was carried out in the presence of a radical scavenger, 2,6-di-*tert*-butyl-*p*-cresol (0.5 equiv.), to retard the formation of thiol radicals. It was observed that in the presence of a radical scavenger, the conversion did not decrease at all. Hence, this radical mechanism is ruled out by our data. Oxidation of thiols is assumed by the second mechanism to occur via reactive Mn(V)-oxo intermediates, which are produced by the reaction of the hydrogen peroxide with Mn(III) and which then react with the thiol in a fashion analogous to that observed previously for the oxidation of sulfides [34]. We tentatively propose the latter mechanism for the oxidation of thiols by  $\text{Fe}_3\text{O}_4@\text{SiO}_2\text{-NH}_2@\text{Mn(III)}$  catalyst (scheme 3).

One of the main objectives of this study was to synthesize a catalyst with high stability and simple reusability. The recyclability of  $\text{Fe}_3\text{O}_4@\text{SiO}_2\text{-NH}_2@\text{Mn(III)}$  nanoparticle as catalyst for the oxidation of thiols was surveyed. In total, six consecutive cycles were carried out. Work-up in between cycles involved the separation of the catalyst particles from the reaction mixture using a magnet and the removal of the clear supernatant solution (figure 6). The catalyst particles were washed several times with  $\text{CH}_2\text{Cl}_2$  and  $\text{CH}_3\text{OH}$ , dried, and then reused in the subsequent cycle. The results show that  $\text{Fe}_3\text{O}_4@\text{SiO}_2\text{-NH}_2@\text{Mn(III)}$  nanocatalyst can be recovered, recycled, and reused more than five times without any deterioration of conversion, selectivity, and magnetic properties (figure 7). In addition, AAS analysis of the supernatant did not show any leaching of manganese species



Scheme 3. Possible mechanisms for the oxidation of thiols by Fe<sub>3</sub>O<sub>4</sub>@SiO<sub>2</sub>-NH<sub>2</sub>@Mn(III).

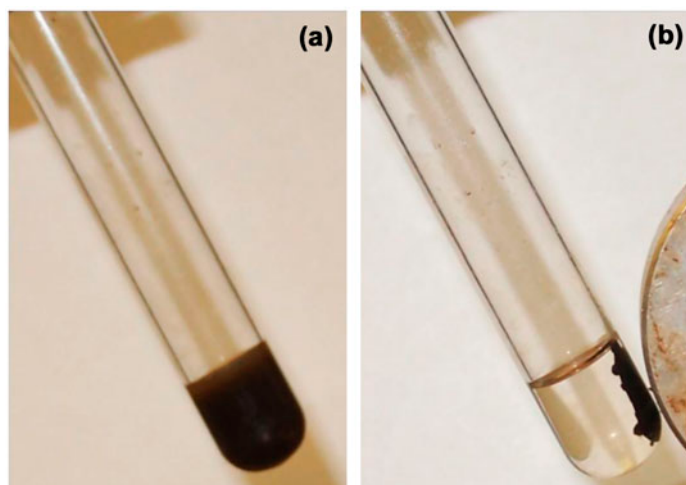


Figure 6. (a) Fe<sub>3</sub>O<sub>4</sub>@SiO<sub>2</sub>-NH<sub>2</sub>@Mn(III) nanocatalyst dispersion in the reaction mixture and (b) Fe<sub>3</sub>O<sub>4</sub>@SiO<sub>2</sub>-NH<sub>2</sub>@Mn(III) nanocatalyst adsorbed on the magnet.

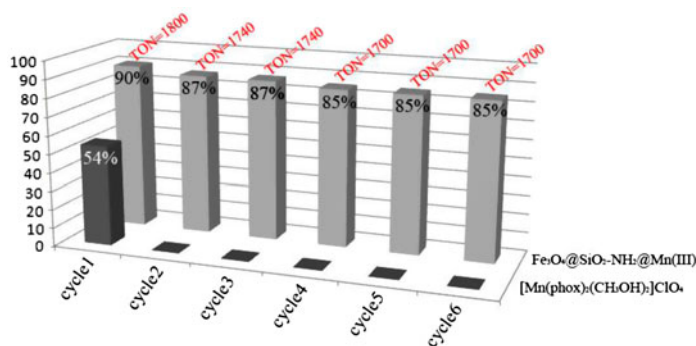


Figure 7. Reuse of [Mn(phox)<sub>2</sub>(CH<sub>3</sub>OH)<sub>2</sub>]ClO<sub>4</sub> (black) and Fe<sub>3</sub>O<sub>4</sub>@SiO<sub>2</sub>-NH<sub>2</sub>@Mn(III) nanocatalyst (gray).

into the solution (detection limit: 0.1 ppm), which indicated that the manganese complex was tightly bound to the surface. A total turnover number of 10,000 is possible after four runs, demonstrating the efficient use of the catalyst in this highly selective reaction (TON=(mol of product)/mol of manganese complex). This is not surprising because the surface -NH<sub>2</sub> shows considerable stability against substitution. On the other hand, all attempts for the separation of homogeneous [Mn(phox)<sub>2</sub>(CH<sub>3</sub>OH)<sub>2</sub>]ClO<sub>4</sub> catalyst from the reaction mixture by solvent extraction method were unsuccessful, another advantage of Fe<sub>3</sub>O<sub>4</sub>@SiO<sub>2</sub>-NH<sub>2</sub>@Mn(III) nanocatalyst over the homogeneous manganese complex.

Comparing our results on thiol oxidation with those of other similar studies [20–29] reveals that the catalyst reported here is superior to some of the previously reported catalysts and reagents in terms of conversions and reaction conditions. In contrast to previously reported work, Fe<sub>3</sub>O<sub>4</sub>@SiO<sub>2</sub>-NH<sub>2</sub>@Mn(III)/UHP does not suffer from drawbacks such as high reaction temperature [27], long reaction time [20], using large amounts of hazardous materials [24, 29], and using stoichiometric amounts of expensive reagents [22, 23, 28]. The attractive features of this catalytic system, such as low cost and simple recyclability, make it particularly suitable for oxidation reactions.

In summary, a method has been presented for the immobilization of a manganese(III) complex on silica-coated MNPs. The nanoparticles can be used as efficient, easily recoverable catalysts for the selective oxidation of thiols to disulfides. With this catalytic system, various thiols were transformed to structurally diverse disulfides in high yields and selectivities. The catalyst particles can be easily collected at the bottom of the test tube using a magnet and reused. The present protocol offers a straightforward path for the immobilization of many other types of catalysts to MNPs, representing a useful alternative to existing catalysts and immobilization methodologies.

## Acknowledgments

We acknowledge the Research Council of Sharif University of Technology for the research funding of this project. Omid Zandi and Meghdad Hosseini are kindly acknowledged for the SEM analysis.

## References

- [1] C.W. Lim, I.S. Lee. *Nano Today*, **5**, 412 (2010).
- [2] S. Shylesh, J. Schweizer, S. Demeshko, V. Schünemann, S. Ernst, W.R. Thiel. *Adv. Synth. Catal.*, **351**, 1789 (2009).
- [3] M.J. Jacinto, R. Landers, L.M. Rossi. *Catal. Commun.*, **10**, 1971 (2009).
- [4] S. Shylesh, W.R. Thiel, V. Schünemann. *Angew. Chem. Int. Ed.*, **49**, 3428 (2010).
- [5] F. Mi, X. Chen, Y. Ma, S. Yin, F. Yuan, H. Zhang. *Chem. Commun.*, **47**, 12804 (2011).
- [6] K. Aranishi, H. Jiang, T. Akita, M. Haruta, Q. Xu. *Nano Res.*, **4**, 1233 (2011).
- [7] Y. Jang, S. Kim, S. Woojoo-Jun, B.H. Kim, S. Hwang, I.K. Song, B.M. Kim, T. Hyeon. *Chem. Commun.*, **47**, 3601 (2011).
- [8] A.K. Tucker-Schwartz, R.L. Garrell. *Chem. Eur. J.*, **16**, 12718 (2010).
- [9] F.-H. Lin, R.-A. Doong. *J. Phys. Chem. C*, **115**, 6591 (2011).
- [10] Y. Sun, G. Liu, H. Gu, T. Huang, Y. Zhang, H. Li. *Chem. Commun.*, **47**, 2583 (2011).
- [11] M. Bagherzadeh, M.M. Haghdooost, A. Shahbazirad. *J. Coord. Chem.*, **65**, 591 (2012).
- [12] H.R. Hoveyda, V. Karunaratne, S.J. Rettig, C. Orvig. *Inorg. Chem.*, **31**, 5408 (1992).
- [13] M. Hoogenraad, K. Ramkisoensing, W.L. Driessen, H. Kooijman, A.L. Spek, E. Bouwman, J.G. Haasnoot, J. Reedijk. *Inorg. Chim. Acta*, **320**, 117 (2001).
- [14] H. Bagheri, O. Zandi, A. Aghakhani. *Anal. Chim. Acta*, **692**, 80 (2011).
- [15] Z. Wang, P. Xiao, B. Shen, N. He. *Colloids Surf., A*, **276**, 116 (2006).
- [16] Z. Jin, W. Tang, J. Zhang, H. Lin, Y. Du. *J. Magn. Magn. Mater.*, **182**, 231 (1998).
- [17] S. Čampelj, D. Makovec, M. Drogenik. *J. Magn. Magn. Mater.*, **321**, 1346 (2009).
- [18] P. Das, A.R. Silva, A.P. Carvalho, J. Pires, C. Freire. *J. Mater. Sci.*, **44**, 2865 (2009).
- [19] All attempts for complete removal of water were unsuccessful.
- [20] C. Tidei, M. Piroddi, F. Galli, C. Santi. *Tetrahedron Lett.*, **53**, 232 (2012).
- [21] L. Menini, M.C. Pereira, A.C. Ferreira, J.D. Fabris, E.V. Gusevskaya. *Appl. Catal., A*, **392**, 151 (2011).
- [22] A. Dewan, U. Bora, D.K. Kakati. *Heteroat. Chem.*, **23**, 231 (2012).
- [23] M. Oba, K. Tanaka, K. Nishiyama, W. Ando. *J. Org. Chem.*, **76**, 4173 (2011).
- [24] C.C. Silveira, S.R. Mendes. *Tetrahedron Lett.*, **48**, 7469 (2007).
- [25] F. Hosseinpour, H. Golchoubian. *Catal. Lett.*, **111**, 165 (2006).
- [26] M. Bagherzadeh, M.M. Haghdooost, M. Amini, P.G. Derakhshandeh. *Catal. Commun.*, **23**, 14 (2012).
- [27] S. Thurow, V.A. Pereira, D.M. Martinez, D. Alves, G. Perin, R.G. Jacob, E.J. Lenardão. *Tetrahedron Lett.*, **52**, 640 (2011).
- [28] H.N. Poa, J.L. Huntinga, R. Mahmuda, R. Radziana, S.-C. Shena. *J. Coord. Chem.*, **51**, 399 (2000).
- [29] S. Raghavan, A. Rajender, S.C. Joseph, M.A. Rasheed. *Synth. Commun.*, **31**, 1477 (2001).
- [30] M. Amini, M. Bagherzadeh, Z. Moradi-Shoeili, D.M. Boghaei, A. Ellern, L.K. Woo. *J. Coord. Chem.*, **66**, 464 (2013).
- [31] M.M. Chau, J.L. Kice. *J. Am. Chem. Soc.*, **98**, 7711 (1976).
- [32] D. Singh, F.Z. Galetto, L.C. Soares, O.E. Dorneles-Rodrigues, A.L. Braga. *Eur. J. Org. Chem.*, **2661**, (2010).
- [33] M.M. Khodaei, I. Mohammadpour-Baltork, K. Nikoofar. *Bull. Korean Chem. Soc.*, **24**, 885 (2003).
- [34] M. Bagherzadeh, R. Latifi, L. Tahsini, M. Amini. *Catal. Commun.*, **10**, 196 (2008).